

Water Resources Research

RESEARCH ARTICLE

10.1029/2021WR030382

Key Points:

- The Yangtze River basin experienced significant vegetation greening during 2001–2018
- The recent vegetation greening led to a significant increase in evapotranspiration (ET)
- Precipitation variability masked the effects of ET increase on water yield

Supporting Information:

Supporting Information may be found in the online version of this article.

Correspondence to:

J. Zhang and C. Song,
zhangjiahao1993@gmail.com;
csong@email.unc.edu

Citation:

Zhang, J., Zhang, Y., Sun, G., Song, C., Li, J., Hao, L., & Liu, N. (2022). Climate variability masked greening effects on water yield in the Yangtze River Basin during 2001–2018. *Water Resources Research*, 58, e2021WR030382. <https://doi.org/10.1029/2021WR030382>







Received 10 MAY 2021

Accepted 18 DEC 2021

Author Contributions:

Conceptualization: Jiehao Zhang, Yulong Zhang, Ge Sun, Conghe Song
Data curation: Jiehao Zhang
Formal analysis: Jiehao Zhang
Investigation: Jiehao Zhang
Methodology: Jiehao Zhang
Software: Jiehao Zhang
Supervision: Ge Sun, Conghe Song, Jiangfeng Li
Validation: Jiehao Zhang, Lu Hao, Ning Liu
Visualization: Jiehao Zhang
Writing – original draft: Jiehao Zhang

Climate Variability Masked Greening Effects on Water Yield in the Yangtze River Basin During 2001–2018

Jiehao Zhang^{1,2} , Yulong Zhang^{2,3} , Ge Sun⁴ , Conghe Song² , Jiangfeng Li¹, Lu Hao⁵ , and Ning Liu⁴ 

¹Department of Land Resources Management, China University of Geosciences, Wuhan, China, ²Department of Geography, University of North Carolina at Chapel Hill, Chapel Hill, NC, USA, ³Institute for a Secure and Sustainable Environment, University of Tennessee, Knoxville, TN, USA, ⁴Eastern Forest Environmental Threat Assessment Center, Southern Research Station, USDA Forest Service, Research Triangle Park, NC, USA, ⁵Key Laboratory of Meteorological Disaster, Ministry of Education (KLME), Nanjing University of Information Science & Technology, Nanjing, China

Abstract Rapid global vegetation greening has been observed for the past two decades, but its implications to the hydrological cycle are not well understood in many regions, including the Yangtze River Basin (YRB). This study used a remote sensing-driven ecosystem model, the Coupled Carbon and Water model, to fully examine the individual and combined hydrological effects of vegetation and climate changes through a series of modeling experiments. During the study period (2001–2018), the vegetation showed a significant greening trend with the mean annual normalized difference vegetation index increasing at a rate of 0.4% per year ($p < 0.001$). In contrast, climate exhibited a marginal wetting trend with annual precipitation increasing at a rate of 6.7 mm/yr ($p = 0.08$). Annual evapotranspiration (ET) in the YRB significantly increased (3.1 mm/yr, $p = 0.01$) primarily due to enhanced ecosystem productivity associated with vegetation greening, rather than climatic factors. However, the enhancement in ET did not lead to a significant decline in total water yield at the YRB scale. The large inter-annual variability of precipitation masked the effects of vegetation greening on water yield. Overall, our study indicated that the recent land “greening up” has accelerated the regional hydrological cycle through increasing ET and resulted in enhanced risks of water resource shortage. Our findings highlighted the close connection between land cover dynamics and hydrological cycle under climate variability in one of the world’s largest river systems. Effective basin water resource management must consider hydrological response to vegetation greening and climate change.

1. Introduction

The Earth as a whole is greening up since the beginning of the 21st century (Chen et al., 2019; Guay et al., 2014; Schaepman et al., 2011; Zhang et al., 2017b; Zhao et al., 2018; Zhu et al., 2016). Vegetation greening has important implications for the biogeochemical and hydrological cycles, particularly evapotranspiration (ET) at multiple scales (Bai et al., 2020; Teuling et al., 2019; Ukkola et al., 2016; Zeng et al., 2018). ET plays a vital role in linking water, energy, and carbon cycles (Jung et al., 2010; Sun, Alstad, et al., 2011; Wang & Dickinson, 2012). Changes in ET due to vegetation greening directly affect water yield from headwater watersheds for large river systems (Jung et al., 2010; Sun, Caldwell, et al., 2011; Zhang et al., 2015). Understanding the cascading effects of vegetation greening on the hydrological cycle is important in integrated watershed management to address contemporary water resources issues in the context of land-use/land-cover change and climate change (Hao et al., 2015; Sun et al., 2006; Y. Li et al., 2018). However, the interactions among climate, vegetation, and water are highly complex, and significant knowledge gaps remain regarding the influence of forest on water yield under a changing climate (IUFRO, 2018), especially at a large scale (Schwarzer, 2021).

Afforestation is the dominant driver of vegetation greening in many regions of the world (Chen et al., 2019), particularly in East Asia and Europe (Buitenwerf et al., 2018; FAO, 2020). However, the main intentions of afforestation are to increase carbon storage and reduce soil erosion while water is rarely considered to be a priority in forest management (IUFRO, 2018). Guiding principles on water-centered forest management have been developed only recently (FAO, 2021). Concerns have emerged from reports that afforestation programs with a sole focus on promoting carbon sequestration (Fang et al., 2018; Ji et al., 2020) and water quality improvement (Fu et al., 2011; Yang et al., 2015) resulted in significant decrease in water yield (Bai et al., 2020; Kim et al., 2014; Li et al., 2018; Teuling et al., 2019).

Serious ecological consequences have been observed when the trade-offs among ecosystem services were not fully considered in large scale afforestation programs. For example, in the Loess Plateau of China, an arid/semi-arid climate region, streamflow significantly decreased largely due to afforestation and ecological restoration (Feng et al., 2016; Liang et al., 2015). Although greening did not alter as much water yield in tropical/sub-tropical regions as in the Loess Plateau (Guo et al., 2008; Tang et al., 2018), hydrological effects of afforestation in tropical/sub-tropical regions manifest with more uncertainties on water availability and people's wellbeing in the context of increasing frequency of extreme weather events as a result of global climate change (Stocker, 2014; Stott, 2016). For example, afforestation with exotic pine species in Nepal caused spring water decline (Lama, 2019). Vegetation greening potentially induced an increased risk of hydrologic drought in a subtropical watershed in southern China (Zhang et al., 2021).

The Yangtze River Basin (YRB) in southern China drains the world's third longest river system. The YRB is one of the areas with the most widespread subtropical forests around the world (FAO, 2020). YRB has a high spatial heterogeneity in terrain, vegetation, land use, and climate. Significant land cover changes (Zhang et al., 2014), vegetation greening (Chen et al., 2019), and climate variability (Qu et al., 2018) have been observed since the late 1990s. The forest coverage of the YRB increased from 29.5% in 2000% to 43.0% in 2020 largely due to a series of large-scale forest conservation and restoration programs (National Forestry and Grassland Administration of China, 2020). Consequently, the YRB experienced more vegetation greening than any other basins with comparable sizes in the world (Chen et al., 2019). Increasingly severe water shortage and flooding in different parts of the YRB were reported in recent years due to an increasing frequency of extreme weather events (Table S1). One example was the most recent 2020 summer flood that seriously affected the livelihoods of 30.2 million people in the basin. The YRB can be a good testbed for investigating the hydrological effects of vegetation greening in the subtropics, providing insights for water resources management under a changing climate for large basins.

Separating the effects of vegetation on watershed hydrology from climate and other factors can be challenging at a large scale. Many remote-sensing-based ecohydrological models have been developed to understand vegetation–water interactions (Mu et al., 2011; Wang & Dickinson, 2012). Based on the methods used in coupling photosynthetic carbon uptake and water loss via transpiration, these models can be generally regrouped as water-centric or carbon-centric models (Zhang, Song, et al., 2016). Most traditional hydrological models are water-centric models that heavily rely on the Penman–Monteith equation to estimate ET with more focus on soil water movement and river flow routing or empirical/semi-empirical equations (e.g., WaSSI, GLEAM) (Martens et al., 2017; Sun, Caldwell, et al., 2011). However, these models often oversimplify the biophysical processes of vegetation without coupling the transpiration processes in response to changes in vegetation characteristics. Therefore, water-centric models lack the rigorous biological constraint of photosynthetic carbon uptake on ET, which is directly affected by vegetation greening. In contrast, vegetation condition and biological processes are emphasized in carbon-centric models. The ET process is mechanistically integrated in modeling carbon uptake in those carbon centric models. Therefore, the carbon-centric models can provide improved and direct biological understanding of the hydrological effects of vegetation greening.

To fill these knowledge gaps and better understand the regional hydrological response to vegetation greening in the YRB, we adapted a remote sensing-driven carbon-centric model (Zhang, Song, et al., 2016, 2019) to estimate ET and water yield (WY) from 2001 to 2018. We hypothesize that the significant vegetation greening during the study period could induce a strong ET increase, thus may cause WY to decrease. Specifically, our study focuses on the following questions: (a) What were the spatial and temporal patterns of vegetation greening and climate change in the YRB during 2001–2018? (b) How did ET and WY change temporally and spatially? and (c) To what extent did vegetation greenness change affect ET and WY? Our overall goal was to improve the understanding of the effects of vegetation greening on water resources for a large basin amid climate change and variability.

2. Methods and Data

2.1. Study Area

The Yangtze River originates from the east of Qinghai-Tibet Plateau and flows into the East China Sea, winding through 19 provinces with a length of over 6,300 km. The Yangtze River Basin (YRB) (24°30' ~ 35°45'N and 90°33' ~ 122°25'E), covers an area of ~1.8 million km², which makes up 18.8% of China's land area (Figure 1). The multi-year average runoff of the YRB is 961.6 km³/yr, ranking the third in the world. The topography of

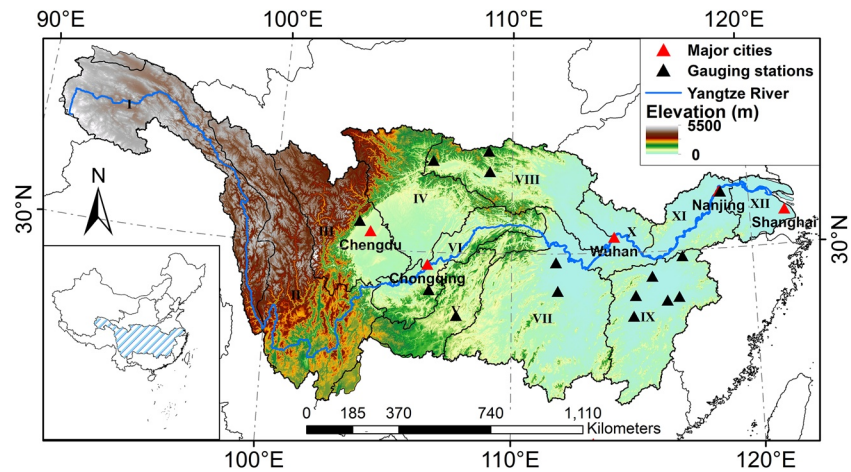


Figure 1. The geographic location and topography of the Yangtze River Basin. The 12 sub-basins include the Upper Jinsha River (I), the Lower Jinsha River (II), the Mintuo River (III), the Jialin River (IV), the Wu River (V), the Upper Mainstream (VI), the Dongting Lake (VII), the Han River (VIII), the Poyang Lake (IX), the Middle Mainstream (X), the Lower Mainstream (XI), and the Tai Lake (XII).

the YRB shows a decreasing complexity from the west to the east, having high landscape heterogeneity from the Tibetan Plateau (over 4000 m a.s.l.) to the relatively flat Yangtze River Delta (below 50 m a.s.l.). Therefore, there are huge variabilities in climate and consequently vegetation communities within the basin. The YRB can be divided into 12 large sub-basins (Figure 1). The YRB resides in a subtropical monsoon climate characterized by distinct four seasons with abundant moisture and heat (Su et al., 2006) except for the Tibetan Plateau (parts of sub-basin I, II). Moreover, the YRB is an important economic region, contributing to 41% of China's gross domestic product and supporting the livelihoods of more than 400 million people (Yang et al., 2015). The water resources in the YRB not only directly influence the sustainability of the economic growth in the region, but also major cities in Northern China through a South-to-North Water Diversion Project to mitigate water shortage.

The YRB experienced large-scale deforestation for timber production, and consequently land degradation during the 1950s–1990s (Wei et al., 2008; Zhang & Song, 2006). From 1957 to 1986, the forest cover of the YRB was reduced by half while soil erosion doubled (Yin & Li, 2001). The disastrous flooding event across the entire YRB in 1998 was the largest flood since 1954, killing more than 4,000 people and causing a direct economic loss of more than US\$20 billion (Zhang et al., 2000). In response, the Chinese government initiated the Natural Forest Conservation Program (NFCP) that banned timber harvesting in natural forests in the upper reaches of YRB (Zhang et al., 2000) and the Conversion of Cropland to Forest Program that encouraged farmers to convert cropland on slopes to forests or grassland (Uchida et al., 2005; Zhang et al., 2017a; Zhang & Song, 2006). These programs significantly increased forest cover in the YRB (Qu et al., 2018; Zhang et al., 2014). During the same period, unprecedented urbanization occurred in the YRB, primarily at the expense of croplands (Kuang & Dou, 2020).

2.2. The Coupled Carbon and Water (CCW) Model

The CCW model is a remote sensing-based data-driven model (Zhang, Song, et al., 2016), which effectively couples carbon and water in a simple framework to estimate gross primary productivity (GPP) and ET at the monthly scale. The CCW is a carbon-centric model, in which ET estimation is constrained by GPP and the underlying water-use efficiency (UWUE) (Zhou et al., 2014). The CCW was calibrated based on global FLUXNET data (Pastorello et al., 2020) and has a much simpler model structure but comparable accuracy with the more complex process-based models for ET (Zhang, Song, et al., 2016, 2019). The key model elements in the CCW include:

$$\text{GPP} = \text{APAR} \times \epsilon = (\text{PAR} \times \text{FPAR}) \times (\epsilon_{\text{pot}} \times R_s) \times (T_s \times W_s) \quad (1)$$

$$\text{ET} = \frac{\text{GPP} \times \text{VPD}^{0.5}}{\text{UWUE}} \quad (2)$$

Table 1
Hydrology, Climate, and Vegetation Data for Model Validation in the Yangtze River Basin

Dataset	Usage	Original resolution (spatial/temporal)	Period	Source
Land cover	Drive model	500 m (Yearly)	2001–2018	MODIS, MCD12Q1 v006
NDVI	Drive model	250 m (16-day)	2001–2018	MODIS, MOD13Q1 v006
Climate ^a	Drive model	~4 km (Monthly)	2001–2018	TerraClimate (http://www.climatologylab.org/terraclimate.html)
Reported streamflow for sub-basins	Model evaluation	Yearly	2001–2018	The Water Resource Bulletin of the Yangtze River Basin
Measured small watersheds streamflow ^b	Model evaluation	Yearly	1986–2019	On-site streamflow records and the regional flow summary reports of government.
Five published ET datasets	Model evaluation	Yearly or Monthly	2001–2014 (or 2015, 2018)	See Table S2 for detailed source information

^aClimate data include precipitation, temperature, vapor pressure deficit, and shortwave radiation. ^bThe periods of measured streamflow for different watersheds vary; more details can be found in Table S3 in the Supporting Information.

where GPP is the Gross Primary Production; APAR is the absorbed photosynthetically active radiation ($\text{MJ}\cdot\text{m}^{-2}$), and PAR is the incident photosynthetically active radiation at the top of vegetation canopy, which is assumed to be 45% of the total shortwave radiation (Running et al., 2000); FPAR is the fraction of PAR absorbed by plants; ϵ_{pot} ($\text{g}\cdot\text{C}/\text{MJ}$) is the potential light use efficiency (LUE) under optimal conditions; R_s , T_s , and W_s are respectively the environmental scalars for diffuse radiation, temperature, and moisture stresses on primary production, each of which takes a value within the range of [0,1]. The UWUE, underlying water use efficiency (Zhou et al., 2014), was derived from FLUXNET data (Pastorello et al., 2020) for each biome. UWUE values range from 4.5 to 8.4 g C/kg H_2O for different biomes. CCW uses biome-specific parameters and is suitable to examine the effects of land cover change on carbon and water balances. More details of the theoretical framework for CCW can be found in Zhang et al. (2016b, 2019).

Here, WY represents the sum of changes in soil water storage and both surface and groundwater flows. We calculate annual WY by subtracting modeled ET from precipitation (P) with an assumption of negligible changes in soil water over a long period (one year or longer):

$$WY = P - ET \quad (3)$$

The YRB was divided into 1,782 watersheds with an average area of around 1000 km^2 for estimating mean WY from gridded WY. The watershed boundaries were derived from the HydroSHEDS dataset, which is a suite of geo-referenced data sets, including river networks, watershed boundaries, drainage directions, and flow accumulations, generated with high-resolution elevation data obtained by NASA's Shuttle Radar Topography Mission (SRTM) (Lehner & Grill, 2013).

2.3. Remote Sensing Data

The land cover data were derived from the MODIS annual 500-m land cover product (i.e., MCD12Q1 v006 dataset) from 2001 to 2018 (Table 1). This dataset was produced based on the 17-class International Geosphere-Biosphere Program (IGBP) classification scheme, processed with a hierarchical classification model where the classes included in each hierarchy reflect structural distinctions of land cover properties (Sulla-Menashe et al., 2019). The biome-specific parameters of CCW were determined based on IGBP land cover classes. To facilitate land cover change analysis, we merged the 17-class IGBP land cover into seven biome types, that is, cropland, forest, shrubland, grassland, urban land, barren land, and water.

The monthly normalized difference vegetation index (NDVI) data were derived from MODIS MOD13Q1 v006 dataset for the same period at 250 m spatial resolution with the sinusoidal projection. MODIS NDVI does not have sensor inconsistency issue like in the coarse-resolution GIMMS3g NDVI product based on AVHRR or the fine scale Landsat NDVI (Land 5/7/8), and its sensor degradation issues in v005 dataset had been satisfactorily

corrected in the v006 (Zhang et al., 2017b). The 1-km NDVI data were smoothed with TIMESAT 3.2 software and upsampled to 500-m resolution based on the cubic convolution resampling method.

2.4. Climate Data

The climate data included precipitation, air temperature, vapor pressure deficit (VPD), and shortwave radiation (SRad). The relevant climate data for 2001 to 2018 (Table 1) were derived from the TerraClimate dataset (Abatzoglou et al., 2018), which is a monthly dataset generated with climatically aided interpolation, combining high-spatial-resolution climatological norms from the WorldClim dataset. Given there was no mean air temperature in the dataset, we calculated it by averaging monthly maximum and minimum temperatures. We validated this dataset with observed precipitation (subbasin scale) and temperature (station scale) before using it as model drivers. TerraClimate precipitation and temperature are strongly consistent with the corresponding observed climate data (R^2 of 0.97 and 0.99 respectively). The original climate datasets were downscaled from a ~ 4 km ($1/24^\circ$) spatial resolution to 500-m with the cubic convolution resampling method.

2.5. Model Evaluation

The original CCW model was calibrated and evaluated based on the global FLUXNET data (Pastorello et al., 2020). To better evaluate the model performance of CCW in the YRB, we further compared CCW ET with five existing ET products, including (a) the Global Land Evaporation Amsterdam Model (GLEAM; version 3.5a) (Martens et al., 2017; Miralles et al., 2011); (b) MOD16A3GF (v006) (Running et al., 2019); (c) the Penman-Monteith-Leuning model (PML_V2) (Zhang, Peña-Arancibia, et al., 2016); (d) the Priestley-Taylor Jet Propulsion Laboratory model (PT-JPL) (Niu et al., 2020); (5) FLUXCOM (Jung et al., 2019). The five ET products are derived with different algorithms, such as Penman-Monteith-based models (MOD16, PML_V2), microwave remote sensing and Priestley-Taylor-based model (GLEAM), remote sensing-based Priestley-Taylor Jet Propulsion Laboratory model (PT-JPL), and FLUXNET data-based machine learning methods (FLUXCOM). We compared CCW ET with the five datasets at both the whole YRB and sub-basin scale. More details about the ET datasets can be found in Table S2.

In addition, we further evaluated CCW ET using water resource records for 12 sub-basins of the YRB (Figure 1) from 2001 to 2018 (Ministry of Water Resources of China, 2019). We calculated annual ET (P-Q method) of sub-basins by subtracting streamflow (Q) from precipitation, assuming that the change in soil water storage is negligible at the annual time step, and then used it to evaluate the annual ET generated by the CCW model. We also assembled streamflow data for 15 relatively small watersheds distributed over a wide range of climate and land cover conditions within the YRB (Hao et al., 2015; Liu et al., 2020) (Figure 1). Given that streamflow data of the 15 small watersheds covered different periods due to differences in data sources, we compared multi-year average CCW ET and streamflow-based ET at the watershed scale. It should be noted that the YRB is a densely populated area where human activities, such as water extraction for domestic use and countless reservoirs for irrigation and hydropower, could greatly influence natural streamflow and thus ET estimates.

2.6. Scenario Designs

To explore the relative contributions of vegetation change and climate change on ET and water yield, we designed two scenario experiments. First, we estimated actual ET and WY by allowing land cover type, NDVI, and climatic variables to change dynamically from 2001 to 2018. The ET and WY changes relative to 2001 in this scenario would be the actual effects of the combined climate and vegetation changes. Second, to quantify the effect of climate alone on ET and WY, we designed an experiment in which we only allowed climate variables to change with time and both LULC and NDVI were fixed at the level of 2001. Thus, the effects of climate on ET (or WY) would be the ET (or WY) in the second scenario relative to 2001. Thereby, the difference between ET (or WY) for the previous two scenarios would be the effects of vegetation change.

To investigate the effects of vegetation change on ET or WY, the linear temporal trend of NDVI and that of ET (or WY) was regressed for vegetation change only and vegetation-climate combined effects, respectively, at the watershed scale. If the change rates of NDVI and ET (or WY) are tightly coupled, vegetation change can be regarded as the dominant factor associated with ET (or WY) change.

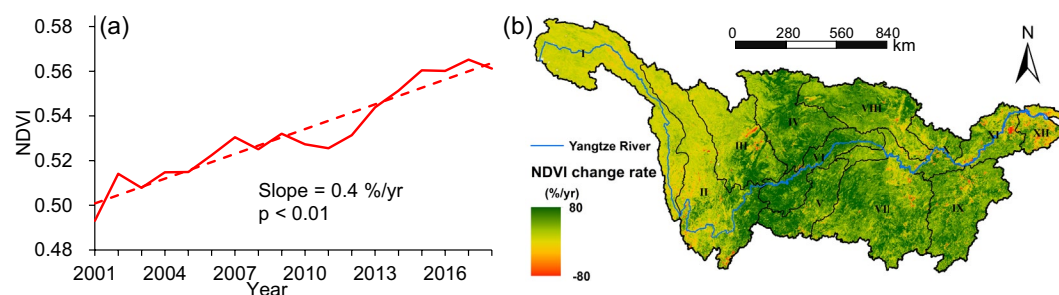


Figure 2. The vegetation change from 2001 to 2018 in the Yangtze River Basin: (a) basin-wide annual normalized difference vegetation index (NDVI) change over time and (b) spatial pattern of NDVI change rate and direction from 2001 to 2018.

3. Results

3.1. Vegetation and Climate Changes During 2001–2018

The annual mean NDVI over the YRB showed a significant upward trend with a rate of 0.4%/yr ($p < 0.01$) (Figure 2a). Spatially, 90.4% of the area exhibited an increasing trend, of which 76.4% showed a significant ($p < 0.05$) increase, mainly distributed in the middle and the eastern upper reaches of the YRB. A small portion of YRB in the lower reaches showed a downward NDVI trend (Figure 2b), which is mainly located in the Yangtze River Delta as a result of urbanization (Gao et al., 2012; Hao et al., 2015, 2018).

Significant land cover changes were observed during the study period. The total area of forest in the YRB increased from 15.6% (278,416 km²) in 2001% to 19.0% (339,069 km²) in 2018 based on MODIS land cover product, and 98.1% of the new increased forests were converted from shrublands. The change in shrubland coverage was relatively small compared to forests. The new shrublands originated from croplands and grasslands (71,472 km² or 4.1% of the YRB), roughly offsetting shrublands' conversion to forests. The new shrublands are likely the early stage forests established through the Conversion of Cropland to Forest Program (Zhang & Song, 2006). Although the total urban land area was small (about 1.9% of the YRB) compared to other land cover types, it increased substantially in relative term by 42.3% during the study period, almost exclusively coming from croplands (45.0%) and grassland (49.6%).

Annual climate (temperature, VPD, and shortwave radiation) did not show any significant trend even at the 90% confidence level during 2001 and 2018, except annual total precipitation showing an increase of 6.7 mm/yr ($p = 0.08$) (Figure S1 in Supporting Information S1). Temperature, VPD, and shortwave radiation all had insignificant trends during 2001–2018 (0.01°C/yr, $p = 0.30$ for temperature; -0.01 hPa/yr, $p = 0.65$ for VPD; -0.06 W/m²/yr, $p = 0.76$ for shortwave radiation) (Figure S1 in Supporting Information S1).

3.2. Model Evaluation

The modeled ET by CCW compared well with existing ET data products. The R^2 values were above 0.7 for four of the five ET products at the whole YRB scale. At the sub-basin scale, CCW ET had an average R^2 of 0.75 with a median of 0.82 for linear regression with the ET products. The CCW ET was relatively close to most of the ET datasets in magnitude. Annual ET rates of the YRB from different sources ranged from 550 to 650 mm (CCW, MODIS, PML_V2, PT-JPL). It appears that ET for GLEAM and FLUXCOM (700–770 mm) was much higher than others, while streamflow-based ET was the lowest (480–580 mm) (Figure 3a).

Among the five ET products, all three ET datasets covering 2001–2018 (MOD16, GLEAM, PML_V2) showed a statistically significant upward trend ($p < 0.05$) (Figure 3a). Similarly, PT-JPL ET that covers 2001–2015 had an upward trend ($p = 0.06$) (Figure 3a). The streamflow-based ET also showed an upward trend in annual ET for the YRB ($p = 0.15$) despite not as strong (Figure 3a). The CCW ET also showed a consistent trend with those of the five ET datasets at the sub-basin scale, with an average R^2 of 0.52 and a median of 0.57.

Compared to streamflow-based ET estimates ($P-Q$) at the sub-basin scale, the CCW ET captured about 64% of its variation ($R^2 = 0.64$) at the annual scale with a minor systematic bias (Figure 3b) and a root mean square error (RMSE) of 127.0 mm for the 12 sub-basins in YRB. The simulated WY is highly consistent with the observed

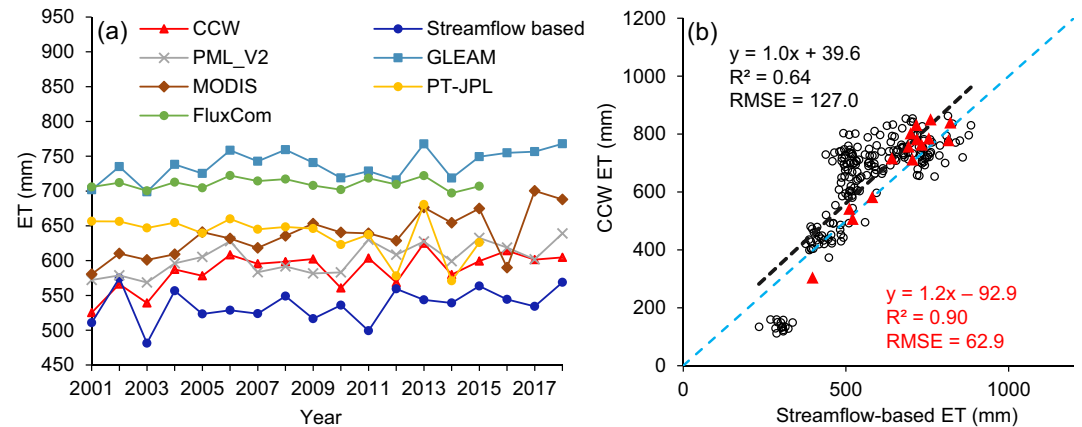


Figure 3. (a) The temporal variation of annual evapotranspiration (ET) for coupled carbon and water (CCW), the five ET products, and the ET derived from streamflow; (b) the comparison between the CCW annual ET with annual ET estimated from water balance-based ET (i.e., precipitation - streamflow) for the 12 sub-basins of the Yangtze River Basin from 2001 to 2018 (black circles) and that for 15 small watersheds on multi-year mean ET (red solid triangles). The blue dashed line in (b) represents the 1:1 line.

streamflow for the whole YRB ($R^2 = 0.91$). The average annual CCW ET compared better with ET estimated by the P-Q method for the 15 small watersheds, with higher R^2 ($=0.90$) and a lower RMSE ($=62.9$ mm) (Figure 3b).

3.3. Effects of Vegetation and Climate Change and Variability on ET

Annual ET in YRB significantly varied spatially, decreasing from the east to the west (Figure 4a). At the sub-basin scale, the average annual ET ranged from 412 mm in sub-basin III to 772 mm in IX except sub-basin I which has a much lower ET than all others (Figure 4a). The annual ET in the YRB significantly increased at a rate of 3.1 mm/yr ($p = 0.01$) under the combined influence of climate and vegetation change from 2001 to 2018 (Figures 4b and Table 2). A positive trend of ET was seen over 80.5% of the basin, where ET increased with an

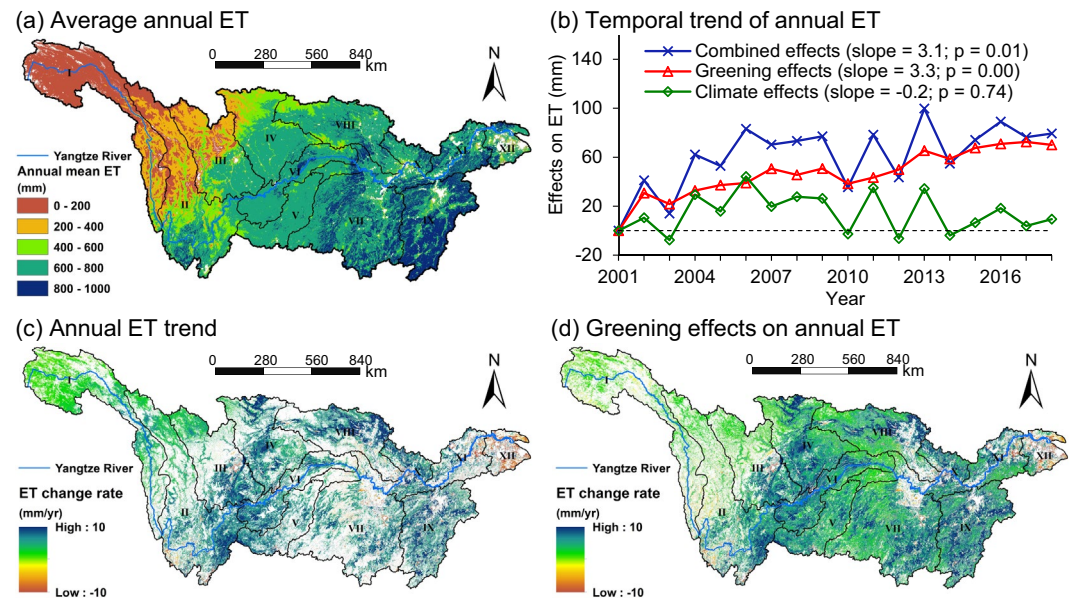


Figure 4. Spatial distribution of the average annual evapotranspiration (ET) of 2001–2018 in the Yangtze River Basin (a); temporal variation of the combined and independent effects of climate and vegetation change on annual ET (b); spatial distribution of linear slope of annual ET (c); and vegetation greening effects on annual ET (d) at the confidence level of 95% ($p < 0.05$) from 2001 to 2018.

Table 2

Summary of the Combined and Individual Effects of Vegetation and Climate Changes on Evapotranspiration (ET) in the Yangtze River Basin (YRB) From 2001 to 2018

Effects	Change rate		ET increased area		ET decreased area	
	mm/yr	<i>p</i>	Slope (mm/yr)	Area proportion (%)	Slope (mm/yr)	Area proportion (%)
Combined	3.1	0.01	4.3	80.5 (40.3)	−0.6	16.0 (3.1)
Climate	−0.2	0.74	1.1	45.8 (6.3)	−0.5	50.0 (1.0)
Vegetation	3.3	<0.01	4.4	81.0 (56.2)	−0.5	15.5 (4.0)

Note. The values in the parentheses are the proportion of areas (%) reaching a statistical significance level ($p < 0.05$).

average rate of 4.3 mm/yr (Table 2). Moreover, ET increased significantly ($p < 0.05$) in 40.3% of the basin (Figures 4c and Table 2). The most significant ET increasing area was in the eastern upper reach and the northern middle reach of the YRB (Figure 4c). In contrast, the plain area of the YRB showed a downward trend, particularly around the metropolitan areas in the Yangtze River Delta (Figure 4c).

The enhancement in ET over the YRB was mainly due to vegetation greening (Figures 4b and 4d). Annual ET had a significant positive trend (3.3 mm/yr or 0.7%/yr, $p < 0.01$) from 2001 to 2018 as a result of vegetation changes (Figures 4b and Table 2). Spatially, 81.0% of the total area showed ET increase from vegetation greening, of which 70% increased significantly ($p < 0.05$) (Figure 4d). Most of the greening-induced ET increase area was found in central and eastern YRB (Figure 4d). Most areas where NDVI increased also had a positive trend in ET with a high spatial correlation ($R = 0.7$, $p < 0.01$) between trends of NDVI and ET for the combined effects (Figure 5a). The correlation was much stronger, when the effects of climate were removed ($R = 0.9$, $p < 0.001$, Figure 5a).

By land cover type, stable vegetation contributed 92.5% of the ET increase. The proportions of stable cropland (13.3%) and forest (13.9%) to the total area are close, but the contribution of the stable forest to ET increase was only 61.1% of that from cropland. The majority of the croplands are rice paddies that have evapotranspiration rate close to potential ET. In contrast, an insignificant trend was attributed to climate (−0.2 mm/yr, $p = 0.8$) from 2001 to 2018 (Figure 4b). A significant ET increase trend ($p < 0.05$) due to climate was observed in only 6.3% of the YRB (Table 2).

ET in the YRB exhibited a strong seasonal pattern with the highest ET in the wet season (June to August) and the lowest in the dry season (December to February) (Figure 6). However, the change rates of monthly ET from greening showed a different pattern among seasons. All months have an increase in ET under the influence of vegetation change alone during 2001–2018. The monthly ET changed most from vegetation greening in the spring and autumn months (i.e., April–May and October–November) with a rate of 0.4–0.6 mm/yr, while the monthly ET in summer (June–August) had a much weaker trend (0.1–0.4 mm/yr) (Figure 6). The change rates and directions of changes in ET for each month were consistent with those of NDVI and even greater than the change rates of NDVI in months other than June to September.

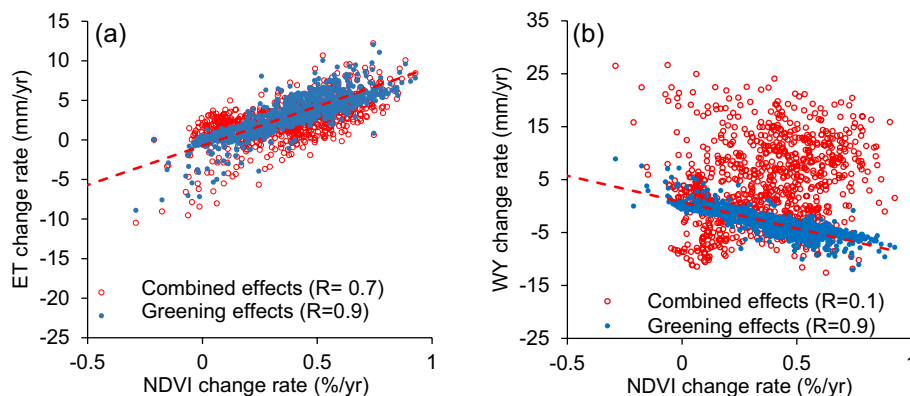


Figure 5. The relationship between the rate of change in evapotranspiration (ET) (a) and water yield (WY) (b) with the rate of change in normalized difference vegetation index (NDVI) at the watershed scale, where each dot represents a watershed, the red dots show the combined effects of climate and vegetation changes on ET (or WY), and the blue dots show the effect of vegetation change alone on ET (or WY).

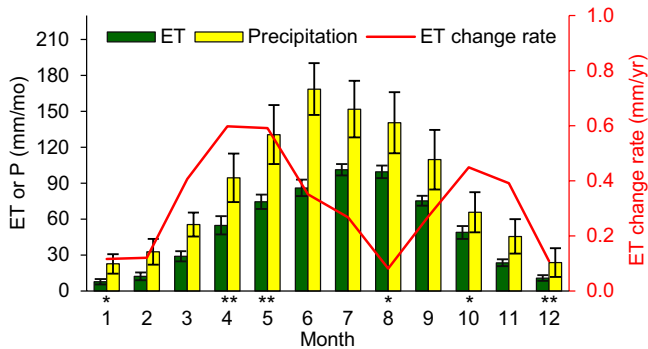


Figure 6. The average monthly evapotranspiration (ET) and precipitation (P) and the monthly ET change rate under the effects of vegetation greening alone during 2001 and 2018 in the Yangtze River Basin. The error bars represent the standard deviation of ET or P. The symbols ** and * represent that the trend of ET is significant ($p < 0.05$) and marginally significant ($p < 0.1$), respectively.

3.4. Effects of Vegetation and Climate Change on WY

The multi-year average WY was 481 mm, accounting for 45.9% of the mean annual precipitation (1,047 mm). Spatially, the highest WY was above 800 mm in the eastern coastal area of the YRB, while the lowest WY was less than 200 mm in the southwest and middle north of the YRB (Figure 7a). At the sub-basin scale, sub-basin VIII (Han River basin) had the lowest WY, which was only 266 mm, while the sub-basin IX (Poyang Lake Basin) had the highest WY (809 mm, Figure 7b). Meanwhile, the sub-basin VIII (Han River basin) also had the lowest WY/P ratio of 0.29 (Figure 7b). The inter-annual variation of WY was almost perfectly correlated with that of P, and the coefficient of correlation between WY and P was above 0.9 for all 1,782 watersheds within the YRB. In contrast, the correlation coefficient of ET and WY was not significant, only -0.3 ($p = 0.19$).

The vegetation change had significant negative effects on WY with a rate of -3.3 mm/yr ($p < 0.01$) (Figure 7d). These negative greening effects on WY were offset by the effects of climate variability, which caused a marginally significant increase in WY, with a rate of 6.8 mm/yr ($p = 0.10$) (Figure 7d).

As a result, annual WY showed an increase with a rate of 3.5 mm/yr ($p = 0.33$) under the combined effects of vegetation and climate from 2001 to 2018 with great inter-annual variations (Figure 7c). Spatially, only a small proportion of the YRB showed a significant ($p < 0.05$) trend in annual WY due to its great fluctuation. The areas where significant urban expansion occurred, for example, Yangtze River delta, showed an increase in WY, while the southwest region showed a decrease in WY.

The cumulative changes in WY from vegetation greening from 2001 to 2018 for the entire YRB were significant in both absolute magnitude and relative percentage. Vegetation greening exerted a negative effect on WY in most of the YRB except a few small areas in the Yangtze River Delta and the southwest (Figure 8). There was a strong correlation ($R = 0.9$, $p < 0.001$) between the change in NDVI and the change in WY (Figure 5b) when the climate effects were excluded. In contrast, such a strong correlation disappeared between the change rate of NDVI and the combined effects on WY (Figure 5b). The effects of climate variation, therefore, masked the effects of vegetation greening on WY. WY in most of the middle and eastern YRB was reduced by more than 50 mm in 17 years

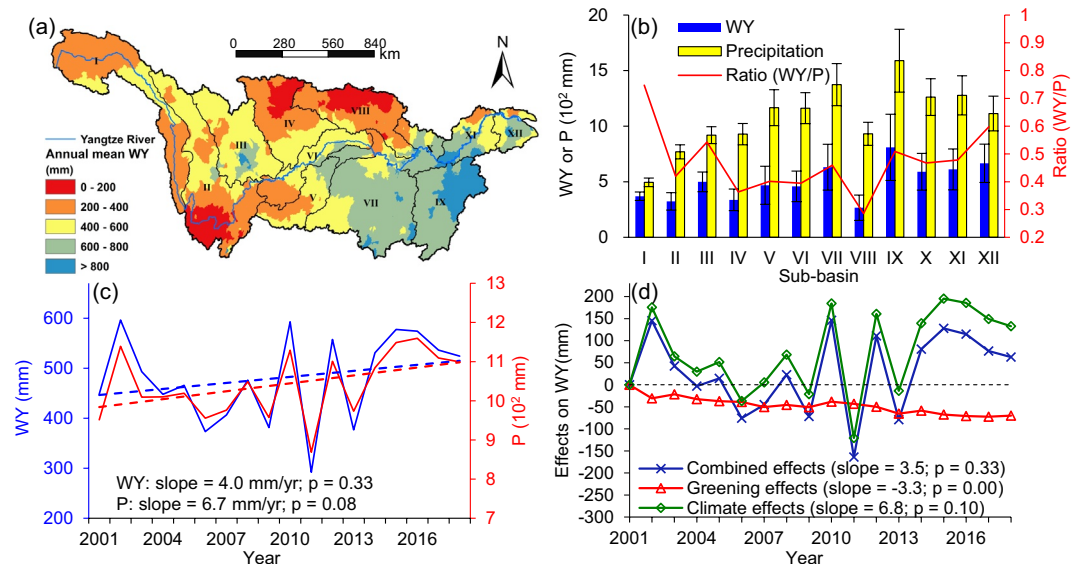


Figure 7. Spatial distribution of average annual water yield (WY) during 2001–2018 in the Yangtze River Basin (a); Annual WY, precipitation (P), and the ratio of WY to P for the 12 sub-basins (b); Temporal variation of annual WY and P during 2001–2018 for the Yangtze River basin (c); Temporal variation of the combined and individual effects of vegetation and climate on annual WY (d).

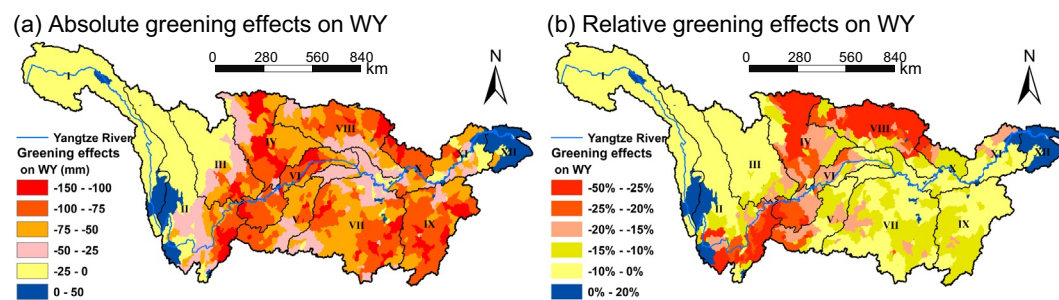


Figure 8. The cumulative absolute (a) and relative (b) effects of vegetation change on water yield (WY) from 2001 to 2018 at watershed-scale.

(Figure 8a). The proportional changes in WY due to greening showed a different spatial pattern (Figure 8b). The middle north and middle west area of the YRB had the most decrease in WY in percentage (Figure 8b). Annual WY decreased above 25% in the middle north area and 15%–25% in the middle west area in 17 years (Figure 8b). The southeast coastal area, where the absolute WY change due to greening was as great as the middle north and middle west, did not show a high proportional decrease in WY from greening because of a much wetter climate. At the sub-basin scale, sub-basin IV and VIII showed the most greening effects on WY in percentage to WY in 2001. WY decreased 78.2 mm due to greening in sub-basin IV (Jialin River basin), accounting for 33% of WY in 2001 (238.2 mm). The greening effects on WY were -74.8 mm in 17 years accounting for 74% of WY in 2001 (93.4 mm) and 26% of the average WY (266.1 mm) in sub-basin VIII (Han River basin, HRB).

4. Discussion

4.1. Greening and ET Rise

Our finding that vegetation greening induced an increase in ET was consistent with previous studies. Many global-scale studies revealed that vegetation greening was the dominant factor of global ET rise (Zeng et al., 2018; Zhang et al., 2015, 2016a). At the continental scale, strong positive correlations ($R > 0.5$) between the trends of ET and LAI were observed in North America, Europe, India, and southern China (Zeng et al., 2018). Teuling et al., (2019) also found that the forest cover increased significantly from 1960 to 2010 in Europe and had positive impacts on ET. The significant ET increase from vegetation greening was also observed in many other areas experiencing greening in China, for example, the Loess Plateau (Shao et al., 2019), and the southern coastal areas (Bai et al., 2020). However, Zhang, Peña-Arancibia, et al. (2016) found that a large proportion of transpiration increase from vegetation greening was offset by its negative effects on soil evaporation in southern China, India and North America, suggesting a large uncertainty in vegetation dynamics and their impacts on water resources in the YRB.

The vegetation greening in the YRB happened through two processes. The first was forest area increase. According to China's National Forest Inventory data (National Forestry and Grassland Administration of China, 2020), forest coverage in YRB increased from 29.5% in 2000% to 43.0% in 2020. The second process was vegetation thickening as indicated by the increase in NDVI for stable vegetated areas. The enhancement of vegetation activity in stable vegetated areas accounted for 75.5% of the increase in annual mean NDVI, while the increase in forest area only contributed 6.7%. Accordingly, the enhancement of vegetation activity (NDVI increase) of the stable vegetation contributed 80.3% of the GPP increase, which resulted in the most crucial contribution (85.7%) to the increase in ET. The rise in greenness for stable vegetation is likely due to the forest conservation and restoration programs initiated in the late 1990s, notably the Natural Forest Conservation Program and Conversion of Cropland to Forest Program (Qu et al., 2018). CO_2 fertilization was also reported as a major driver for global greening (Zhu et al., 2016), and may have contributed to the greening of the stable vegetation in the YRB as well. The significant greening trend induced an increase in GPP with a rate of $12.3 \text{ g C/m}^2/\text{yr}$ (0.9% of the annual GPP in 2001, $p < 0.01$) in the YRB during the study period. Together with the enhancement of vegetation productivity, ET increased significantly, consuming more water as a tradeoff.

Intensification of hydrologic droughts was generally a consequence of increasing ET (Han, Huang, et al., 2020; Padrón et al., 2020; Teuling et al., 2013). Our study showed that vegetation greening had stronger effects on ET

in spring and autumn months (Figure 6), which could potentially exacerbate droughts (Bruijnzeel, 2004; Padrón et al., 2020). In contrast, vegetation greening had minor effects on the intensities of summer droughts (Figure 6).

4.2. Greening Effects on Water Yield

This study found that vegetation greening induced an increase in annual ET significantly by 56 mm from 2001 to 2018 over the YRB, thus decreased WY. This was equivalent to 13% of the annual WY in 2001 (427 mm). The greening effects on WY might be more significant in some local regions. For example, the Han River basin (HRB, VIII) had much less precipitation but similar ET compared to other subtropical sub-basins of the YRB (Figure 7a). Vegetation greening induced an increase in ET by 74.8 mm from 2001 to 2018 in HRB, accounting for 25% of its mean annual WY. The HRB suffered droughts in 2012 and 2013, when enhanced ET from vegetation greening on WY accounted for >60% of the mean WY in the HRB. Thus, the hydrological drought risk might have been significantly enhanced from vegetation greening.

However, we also revealed that climatic factors, especially precipitation, were more important in determining WY in the YRB. The increase and variability of precipitation masked the negative effects of vegetation greening on WY for YRB as a whole. Similar finding was also reported in other areas around the world. For example, in central Sweden, annual streamflow decreased by 39 mm during 1960–2010 due to afforestation, while precipitation induced an increase in streamflow of 67 mm (Teuling et al., 2019), masking the greening effect. In contrast, water yield is more sensitive to vegetation changes in arid/semi-arid areas (Cao et al., 2011, 2016; Feng et al., 2016). For example, vegetation greening and/or afforestation in China's Loess Plateau, an arid/semi-arid area, significantly altered local water availability. In this area, the ratio of annual WY to precipitation decreased from 8% during 1980–1999 to 5% for 2000–2010 as a result of vegetation greening (Feng et al., 2016). It appears that the background climate, watershed size, and magnitude of disturbances are major determinants to the hydrological responses. A global scale study (Zhou et al., 2015) found that climatic factors (precipitation, potential ET), instead of land cover, play the dominant role in hydrological cycle in most of the humid regions. Therefore, the hydrological effects of vegetation greening are most likely masked by the great variability of climatic factors in humid regions of the world. These masked effects are generally missing in records of hydrological gauging stations.

The frequency of extreme weather events significantly increased globally and is predicted to increase in the future due to climate warming (Stocker, 2014; Stott, 2016). On the other hand, ET is relatively stable especially in humid regions such as in the southeastern U.S. according to in-situ data-based studies (Liu et al., 2018; Oishi et al., 2018). Consequently, in meteorological drought periods with precipitation less than normal, the enhanced ET from the increased vegetation cover would aggravate hydrological drought (lower water yield than normal), although its effect is often not strongly seen in years with expected precipitation amount and temporal pattern.

4.3. Implications for Water Management

The large-scale forest conservation and restoration programs play an important role in vegetation greening in China, enhancing carbon sequestration (Chen et al., 2021; Fang et al., 2018; Ji et al., 2020) and mitigating soil erosion (Fu et al., 2011; Yang et al., 2015). Meanwhile, excessive implementation of these programs caused water shortage concerns in the arid regions of northern China (Feng et al., 2016). Our study revealed that the annual ET increase in the YRB was very small relative to precipitation at the large basin scale. However, local and seasonal drought could frequently occur in some parts of the basin, for example, the southwestern region of YRB (Yang et al., 2012). As the frequency and severity of drought and other extreme weather events increase (Stocker, 2014; Stott, 2016), enhanced ET could exacerbate drought impacts (Teuling et al., 2013). Therefore, the effects of afforestation on local WY in the humid regions on water yield should not be neglected.

An improved water resource management plan is needed to deal with effects of the rising ET to mitigate drought impacts in the future. Several forest management measures could be adopted to minimize the impact of forest growth on water resource: (1) avoid using fast growing exotic tree species in afforestation to minimize their water use while still serving soil erosion control and ecological restoration purposes, (2) thin stands to reduce water use, and (3) allow native vegetation to naturally regenerate as a greening strategy other than artificial plantations.

Securing agricultural water supply for irrigation is also critical for drought impact mitigation. The YRB is one of the most important grain production areas in China (Xu et al., 2019). Water availability for irrigation and crop yield is tightly connected. Our study showed a significant ET increase in cropland in the YRB, indicating a rise in agricultural water demand. Globally, cropland contributed one-third of the net increase in leaf area during 2000–2018, ranked the first among all land cover types (Chen et al., 2019). Consequently, the total grain production in the world increased by about 50% from 2000 to 2018 (data from the World Bank, <https://data.worldbank.org/indicator/AG.PRD.CREL.MT>). Irrigation played a critical role in this increase of the grain production (Mueller et al., 2012) in addition to other intensive agricultural management, such as multiple cropping (Ray & Foley, 2013) and increased fertilizer usage (Mueller et al., 2012; Zhang et al., 2018). Thus, water demand for grain production sharply increased. Any fluctuation of water supply for croplands could influence food security. Therefore, local water demand by natural ecosystems and the agricultural sector needs to be considered in the regional sustainable development.

4.4. Research Limitations

There are several limitations in this study that needs to be improved in the future. As a carbon-centric model, CCW ET is tightly associated with carbon uptake (GPP). In the winter months, GPP could be almost zero when vegetation activity ceases. Consequently, ET estimated by CCW would be low as well. However, evaporation would not cease together with transpiration in winter although evaporation is low at this time when evaporation and transpiration decouple. Moreover, UWUE parameters and ET evaluation in the Tibetan Plateau region have more uncertainties than other areas. Few eddy flux sites exist in the FLUXNET dataset for model calibration have a similar environment as the Tibetan Plateau. Besides, the upscaled climate data in the Tibetan Plateau have larger uncertainties due to the sparse distribution of meteorological stations (Li et al., 2014, 2020). Overall, CCW might underestimate ET in the Yangtze River source region and winter months. However, such uncertainties have limited influence on our main conclusions since most of the greening occurred in other parts of the basin.

Our estimate of WY change essentially represents the sum of the change in river flow and soil water storage. A recent study argued that annual WY (or ET) estimated based on water balance has great uncertainties due to the dynamic nature of soil moisture, especially in arid/semi-arid and sparsely vegetated areas (Han, Yang, et al., 2020). However, the water balance-based WY in the humid and densely vegetated areas (e.g., the YRB) has a minor deviation of less than 10% (Han, Yang, et al., 2020). Studies on water storage of the YRB also revealed that the inter-annual variation of water storage for the whole YRB was mostly below 20 mm (Huang et al., 2013; Long et al., 2015). Overall, we believe water balance-based WY estimation in our study is reliable at the YRB. However, future studies on vegetation effects for specific watersheds and different stage of the greening processes may need to consider variations in soil water storage and river flow separately.

Some limitations may come from the data used. We noted that the streamflow-based ET for model evaluation for the sub-basins V and VI (Figure 3b) was only around 500 mm, which was likely too low for subtropical forested areas. These streamflow data used to estimate ET were not the original records from the gauging stations but from government summary reports (Ministry of Water Resources of China, 2019). Combined with uncertainties from countless human activities, future studies should not solely rely on streamflow data for model evaluation. Parameters of CCW were calibrated with data from FLUXNET (Pastorello et al., 2020) for uniform biomes. However, many modeling units are mixtures of multiple biomes to varying degrees. Therefore, biome-specific parameters may cause uncertainty for ET estimation in the area with mixed biomes. In addition, land cover products are often inconsistent (Hua et al., 2018; Ran et al., 2010; Wu et al., 2008). For example, the total forest cover of the YRB in MCD12Q1 v006 (16%–19%) is much lower than that of v005 (25%–35%) (Zhang et al., 2014) as a result of the algorithm used in v006 that imposes stronger constraints on the amount of tree cover (Sulla-Menashe et al., 2019). Adoption of ensemble land cover data from multi-sources could be a way for improvement in the future study.

5. Conclusions

This study examined the individual and combined effects of vegetation and climate changes on terrestrial ET and water yield (WY) with a process-based, carbon-centric, remote sensing-driven model in the Yangtze River Basin (YRB) from 2001 to 2018. We detected a significant vegetation greening trend in the YRB, likely a result of ecological conservation and restoration, cropland productivity improvement, as well as climatic changes. We found

that annual ET increased significantly due to strong vegetation greening, but not climate. However, the enhanced ET did not significantly alter annual water yield at the YRB scale due to the large interannual variability of precipitation. Our study implies that vegetation greening has the potential to cause significant water supply decline, especially in dry seasons and years in relatively dry sub-watersheds. This study suggests that climate variability could mask the greening effects on water yield in large basins. Disaggregating the effects of vegetation greening and climate change on ET and WY provides more specific information for watershed management to mitigate threats to water resource security. Future monitoring studies on the effects of vegetation on watershed hydrology should focus on not only streamflow measurements at the watershed outlets but also on ET processes within the watersheds under a changing climate.

Data Availability Statement

Datasets used for driving the model and modeling results evaluation were obtained from numerous sources as described in Table 1. All the experimental data of this study can be found at <https://osf.io/c8ysg/>.

Acknowledgments

This study was partially supported by the overseas' study scholarship offered by the China University of Geosciences, Wuhan and the National Natural Science Foundation of China (Grants 41877151). The majority of the research was conducted in the Remote Sensing and Ecological Modeling Group in the Department of Geography at the University of North Carolina at Chapel Hill, USA. The Southern Research Station, USDA Forest Service also provided partial support to this research.

References

- Abatzoglou, J. T., Dobrowski, S. Z., Parks, S. A., & Hegewisch, K. C. (2018). TerraClimate, a high-resolution global dataset of monthly climate and climatic water balance from 1958–2015. *Scientific Data*, 5(1), 170191. <https://doi.org/10.1038/sdata.2017.191>
- Bai, P., Liu, X., Zhang, Y., & Liu, C. (2020). Assessing the impacts of vegetation greenness change on evapotranspiration and water yield in China. *Water Resources Research*, 56, 0–2. <https://doi.org/10.1029/2019WR027019>
- Bruijnzeel, L. A. (2004). Hydrological functions of tropical forests: Not seeing the soil for the trees? *Agriculture, Ecosystems & Environment*, 104, 185–228. <https://doi.org/10.1016/j.agee.2004.01.015>
- Buitenwerf, R., Sandel, B., Normand, S., Mimet, A., & Svenning, J.-C. (2018). Land surface greening suggests vigorous woody regrowth throughout European semi-natural vegetation. *Global Change Biology*, 24(12), 5789–5801. <https://doi.org/10.1111/GCB.14451>
- Cao, S., Chen, L., Shankman, D., Wang, C., Wang, X., & Zhang, H. (2011). Excessive reliance on afforestation in China's arid and semi-arid regions: Lessons in ecological restoration. *Earth-Science Reviews*, 104(4), 240–245. <https://doi.org/10.1016/j.earscirev.2010.11.002>
- Cao, S., Zhang, J., Chen, L., & Zhao, T. (2016). Ecosystem water imbalances created during ecological restoration by afforestation in China, and lessons for other developing countries. *Journal of Environmental Management*, 183, 843–849. <https://doi.org/10.1016/j.jenvman.2016.07.096>
- Chen, C., Park, T., Wang, X., Piao, S., Xu, B., Chaturvedi, R. K., & Fuchs, R. (2019). China and India lead in greening of the world through land-use management. *Nature Sustainability*, 2(2), 122–129. <https://doi.org/10.1038/s41893-019-0220-7>
- Chen, S., Zhang, Y., Wu, Q., Liu, S., Song, C., Xiao, J., et al. (2021). Vegetation structural change and CO₂ fertilization more than offset gross primary production decline caused by reduced solar radiation in China. *Agricultural and Forest Meteorology*, 296, 108207. <https://doi.org/10.1016/j.agrformet.2020.108207>
- Fang, J., Yu, G., Liu, L., Hu, S., & Chapin, F. S. (2018). Climate change, human impacts, and carbon sequestration in China. *Proceedings of the National Academy of Sciences of the United States of America*, 115(16), 4015–4020. <https://doi.org/10.1073/pnas.1700304115>
- FAO. (2020). *Global forest resources assessment 2020*. Main report. Food and Agriculture Organization of the United Nations (FAO, Vol. 163). <https://doi.org/10.4060/ca9825en>
- FAO, USDA, IUFRO. (2021). *A guide to forest–water management*. FAO, USDA and IUFRO. <https://doi.org/10.4060/cb6473en>
- Feng, X., Fu, B., Piao, S., Wang, S., Ciais, P., Zeng, Z., et al. (2016). Revegetation in China's Loess Plateau is approaching sustainable water resource limits. *Nature Climate Change*, 6(11), 1019–1022. <https://doi.org/10.1038/nclimate3092>
- Fu, B., Liu, Y., Lü, Y., He, C., Zeng, Y., & Wu, B. (2011). Assessing the soil erosion control service of ecosystems change in the Loess Plateau of China. *Ecological Complexity*, 8(4), 284–293. <https://doi.org/10.1016/j.ecocom.2011.07.003>
- Gao, F., de Colstoun, E. B., Ma, R., Weng, Q., Masek, J. G., Chen, J., et al. (2012). Mapping impervious surface expansion using medium-resolution satellite image time series: A case study in the Yangtze River delta, China. *International Journal of Remote Sensing*, 33(24), 7609–7628. <https://doi.org/10.1080/01431161.2012.700424>
- Guay, K. C., Beck, P. S. A., Berner, L. T., Goetz, S. J., Baccini, A., & Buermann, W. (2014). Vegetation productivity patterns at high northern latitudes: A multi-sensor satellite data assessment. *Global Change Biology*, 20(10), 3147–3158. <https://doi.org/10.1111/gcb.12647>
- Guo, H., Hu, Q., & Jiang, T. (2008). Annual and seasonal streamflow responses to climate and land-cover changes in the Poyang Lake basin, China. *Journal of Hydrology*, 355(1–4), 106–122. <https://doi.org/10.1016/j.jhydrol.2008.03.020>
- Han, J., Yang, Y., Roderick, M. L., McVicar, T. R., Yang, D., Zhang, S., & Beck, H. E. (2020). Assessing the steady-state assumption in water balance calculation across global catchments. *Water Resources Research*, 56(7), e2020WR027392. <https://doi.org/10.1029/2020WR027392>
- Han, Z., Huang, S., Huang, Q., Bai, Q., Leng, G., Wang, H., et al. (2020). Effects of vegetation restoration on groundwater drought in the Loess Plateau, China. *Journal of Hydrology*, 591, 125566. <https://doi.org/10.1016/j.jhydrol.2020.125566>
- Hao, L., Huang, X., Qin, M., Liu, Y., Li, W., & Sun, G. (2018). Ecohydrological processes explain urban dry island effects in a wet region, southern China. *Water Resources Research*, 54(9), 6757–6771. <https://doi.org/10.1029/2018WR023002>
- Hao, L., Sun, G., Liu, Y., Wan, J., Qin, M., Qian, H., et al. (2015). Urbanization dramatically altered the water balances of a paddy field dominated basin in Southern China. *Hydrology and Earth System Sciences Discussions*, 12(2), 1941–1972. <https://doi.org/10.5194/hessd-12-1941-2015>
- Hua, T., Zhao, W., Liu, Y., Wang, S., & Yang, S. (2018). Spatial consistency assessments for global land-cover datasets: A comparison among GLC2000, CCI LC, MCD12, GLOBCOVER and GLCNMO. *Remote Sensing*, 10(11), 1846. <https://doi.org/10.3390/rs10111846>
- Huang, Y., Salama, M. S., Krol, M. S., van der Velde, R., Hoekstra, A. Y., Zhou, Y., & Su, Z. (2013). Analysis of long-term terrestrial water storage variations in the Yangtze River basin. *Hydrology and Earth System Sciences*, 17(5), 1985–2000. <https://doi.org/10.5194/hess-17-1985-2013>
- IUFRO. (2018). *Forest and water on a changing planet: Vulnerability, adaptation and governance opportunities: A global assessment report*. International Union of Forest Research Organizations (IUFRO). Retrieved from <https://edepot.wur.nl/457203>
- Ji, Y., Zhou, G., Luo, T., Dan, Y., Zhou, L., & Lv, X. (2020). Variation of net primary productivity and its drivers in China's forests during 2000–2018. *Forest Ecosystems*, 7(1), 1–11. <https://doi.org/10.1186/s40663-020-00229-0>

- Jung, M., Koirala, S., Weber, U., Ichii, K., Gans, F., Camps-Valls, G., et al. (2019). The FLUXCOM ensemble of global land-atmosphere energy fluxes. *Scientific Data*, 6(1), 1–14. <https://doi.org/10.1038/s41597-019-0076-8>
- Jung, M., Reichstein, M., Ciais, P., Seneviratne, S. I., Sheffield, J., Goulden, M. L., et al. (2010). Recent decline in the global land evapotranspiration trend due to limited moisture supply. *Nature*, 467(7318), 951–954. <https://doi.org/10.1038/nature09396>
- Kim, Y., Band, L. E., & Song, C. (2014). The influence of forest regrowth on the stream discharge in the North Carolina Piedmont watersheds. *JAWRA Journal of the American Water Resources Association*, 50(1), 57–73. <https://doi.org/10.1111/jawr.12115>
- Kuang, W., & Dou, Y. (2020). Investigating the patterns and dynamics of urban green space in China's 70 major cities using satellite remote sensing. *Remote Sensing*, 12(12). <https://doi.org/10.3390/rs12121929>
- Lama, T. (2019). *Nepal has too many pines and it's not a good thing*. The Kathmandu Post.
- Lehner, B., & Grill, G. (2013). Global river hydrography and network routing: Baseline data and new approaches to study the world's large river systems. *Hydrological Processes*, 27(15), 2171–2186. <https://doi.org/10.1002/hyp.9740>
- Li, D., Yang, K., Tang, W., Li, X., Zhou, X., & Guo, D. (2020). Characterizing precipitation in high altitudes of the western Tibetan plateau with a focus on major glacier areas. *International Journal of Climatology*, 40(12). <https://doi.org/10.1002/joc.6509>
- Li, X., Wang, L., Chen, D., Yang, K., & Wang, A. (2014). Seasonal evapotranspiration changes (1983–2006) of four large basins on the Tibetan Plateau. *Journal of Geophysical Research: Atmospheres*, 119(23). <https://doi.org/10.1002/2014JD022380>
- Li, Y., Piao, S., Li, L. Z. X., Chen, A., Wang, X., Ciais, P., et al. (2018). Divergent hydrological response to large-scale afforestation and vegetation greening in China. *Science Advances*, 4(5), eaar4182. <https://doi.org/10.1126/sciadv.aar4182>
- Liang, W., Bai, D., Wang, F., Fu, B., Yan, J., Wang, S., et al. (2015). Quantifying the impacts of climate change and ecological restoration on streamflow changes based on a Budyko hydrological model in China's Loess Plateau. *Water Resources Research*, 51(8), 6500–6519. <https://doi.org/10.1002/2014WR016589>
- Liu, N., Sun, P., Caldwell, P. v., Harper, R., Liu, S., & Sun, G. (2020). Trade-off between watershed water yield and ecosystem productivity along elevation gradients on a complex terrain in southwestern China. *Journal of Hydrology*, 590, 125449. <https://doi.org/10.1016/j.jhydrol.2020.125449>
- Liu, X., Sun, G., Mitra, B., Noormets, A., Gavazzi, M. J., Domec, J. C., et al. (2018). Drought and thinning have limited impacts on evapotranspiration in a managed pine plantation on the southeastern United States coastal plain. *Agricultural and Forest Meteorology*, 262, 14–23. <https://doi.org/10.1016/j.agrformet.2018.06.025>
- Long, D., Yang, Y., Wada, Y., Hong, Y., Liang, W., Chen, Y., et al. (2015). Deriving scaling factors using a global hydrological model to restore GRACE total water storage changes for China's Yangtze River Basin. *Remote Sensing of Environment*, 168, 177–193. <https://doi.org/10.1016/j.rse.2015.07.003>
- Martens, B., Miralles, D. G., Lievens, H., van der Schalie, R., de Jeu, R. A. M., Fernández-Prieto, D., et al. (2017). GLEAM v3: Satellite-based land evaporation and root-zone soil moisture. *Geoscientific Model Development*, 10(5), 1903–1925. <https://doi.org/10.5194/gmd-10-1903-2017>
- Ministry of Water Resources of China. (2019). *The Water Resource Bulletin of the Yangtze River Basin (2001–2019)*, Wuhan.
- Miralles, D. G., Holmes, T. R. H., de Jeu, R. A. M., Gash, J. H., Meesters, A. G. C. A., & Dolman, A. J. (2011). Global land-surface evaporation estimated from satellite-based observations. *Hydrology and Earth System Sciences*, 15(2), 453–469. <https://doi.org/10.5194/hess-15-453-2011>
- Mu, Q., Zhao, M., & Running, S. W. (2011). Improvements to a MODIS global terrestrial evapotranspiration algorithm. *Remote Sensing of Environment*, 115(8), 1781–1800. <https://doi.org/10.1016/j.rse.2011.02.019>
- Mueller, N. D., Gerber, J. S., Johnston, M., Ray, D. K., Ramankutty, N., & Foley, J. A. (2012). Closing yield gaps through nutrient and water management. *Nature*, 490(7419), 254–257. <https://doi.org/10.1038/nature11420>
- National Forestry and Grassland Administration of China. (2020). *China forest resources report (2014–2018)*. Beijing: China Forestry Press
- Niu, Z., He, H., Zhu, G., Ren, X., Zhang, L., & Zhang, K. (2020). A spatial-temporal continuous dataset of the transpiration to evapotranspiration ratio in China from 1981–2015. *Scientific Data*, 7(1), 1–13. <https://doi.org/10.1038/s41597-020-00693-x>
- Oishi, A. C., Miniati, C. F., Novick, K. A., Brantley, S. T., Vose, J. M., & Walker, J. T. (2018). Warmer temperatures reduce net carbon uptake, but do not affect water use, in a mature southern Appalachian forest. *Agricultural and Forest Meteorology*, 252, 269–282. <https://doi.org/10.1016/j.agrformet.2018.01.011>
- Padrón, R. S., Gudmundsson, L., Decharme, B., Ducharme, A., Lawrence, D. M., Mao, J., et al. (2020). Observed changes in dry-season water availability attributed to human-induced climate change. *Nature Geoscience*, 13(7), 477–481. <https://doi.org/10.1038/s41561-020-0594-1>
- Pastorello, G., Trotta, C., Canfora, E., Chu, H., Christianson, D., Cheah, Y. W., et al. (2020). The FLUXNET2015 dataset and the ONEFlux processing pipeline for eddy covariance data. *Scientific Data*, 7(1), 225. <https://doi.org/10.1038/s41597-020-0534-3>
- Qu, S., Wang, L., Lin, A., Zhu, H., & Yuan, M. (2018). What drives the vegetation restoration in Yangtze River basin, China: Climate change or anthropogenic factors? *Ecological Indicators*, 90(March), 438–450. <https://doi.org/10.1016/j.ecolind.2018.03.029>
- Ran, Y., Li, X., & Lu, L. (2010). Evaluation of four remote sensing based land cover products over China. *International Journal of Remote Sensing*, 31(2), 391–401. <https://doi.org/10.1080/01431160902893451>
- Ray, D. K., & Foley, J. A. (2013). Increasing global crop harvest frequency: Recent trends and future directions. *Environmental Research Letters*, 8(4). <https://doi.org/10.1088/1748-9326/8/4/044041>
- Running, S. W., Mu, Q., Zhao, M., & Moreno, A. (2019). *MODIS Global Terrestrial Evapotranspiration (ET) Product (MOD16A2/A3 and Year-End Gap-Filled MOD16A2GF/A3GF) NASA Earth Observing System MODIS Land Algorithm (For Collection 6)*. Washington, DC: National Aeronautics and Space Administration
- Running, S. W., Thornton, P. E., Nemani, R., & Glassy, J. M. (2000). Global terrestrial gross and net primary productivity from the Earth observing system. In *Methods in ecosystem science* (pp. 44–57). Springer. https://doi.org/10.1007/978-1-4612-1224-9_4
- Schaeppman, M. E., de Jong, R., de Bruin, S., de Wit, A., Schaeppman, M. E., & Dent, D. L. (2011). Analysis of monotonic greening and browning trends from global NDVI time-series. *Remote Sensing of Environment*, 115, 692–702. <https://doi.org/10.1016/j.rse.2010.10.011>
- Schwarzer, S. (2021). *Working with plants, soils and water to cool the climate and rehydrate Earth's landscapes*. United Nations Environment Programme. Retrieved from <https://wesr.unep.org/foresight>
- Shao, R., Zhang, B., Su, T., Long, B., Cheng, L., Xue, Y., & Yang, W. (2019). Estimating the increase in regional evaporative water consumption as a result of vegetation restoration over the Loess Plateau, China. *Journal of Geophysical Research: Atmospheres*, 2019JD031295. <https://doi.org/10.1029/2019JD031295>
- Stocker, T. (2014). *Climate change 2013: The physical science basis: Working Group I contribution to the fifth assessment report of the intergovernmental panel on climate change*. Cambridge university Press.
- Stott, P. (2016). How climate change affects extreme weather events: Research can increasingly determine the contribution of climate change to extreme events such as droughts. *Proceedings of the National Academy of Sciences of the United States of America*, 352, 1517–1518. <https://doi.org/10.1126/SCIENCE.AAF7271>

- Su, B. D., Jiang, T., & Jin, W. B. (2006). Recent trends in observed temperature and precipitation extremes in the Yangtze River basin, China. *Theoretical and Applied Climatology*, 83(1–4), 139–151. <https://doi.org/10.1007/s00704-005-0139-y>
- Sulla-Menashe, D., Gray, J. M., Abercrombie, S. P., & Friedl, M. A. (2019). Hierarchical mapping of annual global land cover 2001 to present: The MODIS Collection 6 Land Cover product. *Remote Sensing of Environment*, 222, 183–194. <https://doi.org/10.1016/j.rse.2018.12.013>
- Sun, G., Alstad, K., Chen, J., Chen, S., Ford, C. R., Lin, G., et al. (2011). A general predictive model for estimating monthly ecosystem evapotranspiration. *Ecohydrology*, 4(2), 245–255. <https://doi.org/10.1002/eco.194>
- Sun, G., Caldwell, P., Noormets, A., McNulty, S. G., Cohen, E., Moore Myers, J., et al. (2011). Upscaling key ecosystem functions across the conterminous United States by a water-centric ecosystem model. *Journal of Geophysical Research*, 116, G00J05. <https://doi.org/10.1029/2010JG001573>
- Sun, G., Zhou, G., Zhang, Z., Wei, X., McNulty, S. G., & Vose, J. M. (2006). Potential water yield reduction due to forestation across China. *Journal of Hydrology*, 328(3–4), 548–558. <https://doi.org/10.1016/j.jhydrol.2005.12.013>
- Tang, L.-L., Cai, X.-B., Gong, W.-S., Lu, J.-Z., Chen, X.-L., Lei, Q., & Yu, G.-L. (2018). Increased vegetation greenness aggravates water conflicts during lasting and intensifying drought in the Poyang Lake watershed, China. *Forests*, 9(1), 24. <https://doi.org/10.3390/f9010024>
- Teuling, A. J., de Badts, E. A. G., Jansen, F. A., Fuchs, R., Buitink, J., Hoek van Dijke, A. J., & Sterling, S. M. (2019). Climate change, reforestation/afforestation, and urbanization impacts on evapotranspiration and streamflow in Europe. *Hydrology and Earth System Sciences*, 23(9), 3631–3652. <https://doi.org/10.5194/hess-23-3631-2019>
- Teuling, A. J., van Loon, A. F., Seneviratne, S. I., Lehner, I., Aubinet, M., Heinesch, B., et al. (2013). Evapotranspiration amplifies European summer drought. *Geophysical Research Letters*, 40(10), 2071–2075. <https://doi.org/10.1002/grl.50495>
- Uchida, E., Xu, J., & Rozelle, S. (2005). Grain for green: Cost-effectiveness and sustainability of China's conservation set-aside program. *Land Economics*, 81(2), 247–264. <https://doi.org/10.3368/le.81.2.247>
- Ukkola, A. M., Prentice, I. C., Keenan, T. F., van Dijk, A. I. J. M., Viney, N. R., Myneni, R. B., & Bi, J. (2016). Reduced streamflow in water-stressed climates consistent with CO2 effects on vegetation. *Nature Climate Change*, 6(1), 75–78. <https://doi.org/10.1038/nclimate2831>
- Wang, K., & Dickinson, R. E. (2012). A review of global terrestrial evapotranspiration: Observation, modeling, climatology, and climatic variability. *Reviews of Geophysics*, 50(2). <https://doi.org/10.1029/2011RG000373>
- Wei, X., Sun, G., Liu, S., Jiang, H., Zhou, G., & Dai, L. (2008). The forest-streamflow relationship in China: A 40-year Retrospect 1. *Journal of the American Water Resources Association*, 44(5), 1076–1085. <https://doi.org/10.1111/j.1752-1688.2008.00237.x>
- Wu, W., Shibasaki, R., Yang, P., Ongaro, L., Zhou, Q., & Tang, H. (2008). Validation and comparison of 1 km global land cover products in China. *International Journal of Remote Sensing*, 29(13), 3769–3785. <https://doi.org/10.1080/01431160701881897>
- Xu, X., Hu, H., Tan, Y., Yang, G., Zhu, P., & Jiang, B. (2019). Quantifying the impacts of climate variability and human interventions on crop production and food security in the Yangtze River Basin, China, 1990–2015. *The Science of the Total Environment*, 665, 379–389. <https://doi.org/10.1016/j.scitotenv.2019.02.118>
- Yang, J., Gong, D., Wang, W., Hu, M., & Mao, R. (2012). Extreme drought event of 2009/2010 over southwestern China. *Meteorology and Atmospheric Physics*, 115(3–4), 173–184. <https://doi.org/10.1007/s00703-011-0172-6>
- Yang, S., Xu, K. H., Milliman, J. D., Yang, H. F., & Wu, C. S. (2015). Decline of Yangtze River water and sediment discharge: Impact from natural and anthropogenic changes. *Scientific Reports*, 5. <https://doi.org/10.1038/srep12581>
- Yin, H., & Li, C. (2001). Human impact on floods and flood disasters on the Yangtze River. *Geomorphology*, 41(2–3), 105–109. [https://doi.org/10.1016/S0169-555X\(01\)00108-8](https://doi.org/10.1016/S0169-555X(01)00108-8)
- Zeng, Z., Peng, L., & Piao, S. (2018). Response of terrestrial evapotranspiration to Earth's greening. *Current Opinion in Environmental Sustainability*, 33, 9–25. <https://doi.org/10.1016/j.cosust.2018.03.001>
- Zhang, J., Balković, J., Azevedo, L. B., Skalský, R., Bouwman, A. F., Xu, G., et al. (2018). Analyzing and modelling the effect of long-term fertilizer management on crop yield and soil organic carbon in China. *The Science of the Total Environment*, 627, 361–372. <https://doi.org/10.1016/j.scitotenv.2018.01.090>
- Zhang, K., Kimball, J. S., Nemani, R. R., Running, S. W., Hong, Y., Gourley, J. J., & Yu, Z. (2015). Vegetation greening and climate change promote multidecadal rises of global land evapotranspiration. *Scientific Reports*, 5(1) 15956. <https://doi.org/10.1038/srep15956>
- Zhang, M., Liu, N., Harper, R., Li, Q., Liu, K., Wei, X., et al. (2017). A global review on hydrological responses to forest change across multiple spatial scales: Importance of scale, climate, forest type and hydrological regime. *Journal of Hydrology*, 546, 44–59. <https://doi.org/10.1016/j.jhydrol.2016.12.040>
- Zhang, P., Shao, G., Zhao, G., le Master, D. C., Parker, G. R., Dunning, J. B., & Li, Q. (2000). China's forest policy for the 21st century. *Science*, 288, 2135–2136. <https://doi.org/10.1126/science.288.5474.2135>
- Zhang, Y., Peña-Arancibia, J. L., McVicar, T. R., Chiew, F. H. S., Vaze, J., Liu, C., et al. (2016). Multi-decadal trends in global terrestrial evapotranspiration and its components. *Scientific Reports*, 6(1), 1–12. <https://doi.org/10.1038/srep19124>
- Zhang, Y., & Song, C. (2006). Impacts of afforestation, deforestation, and reforestation on forest cover in China from 1949 to 2003. *Journal of Forestry*, 104, 383–387. <https://doi.org/10.1093/JOF/104.7.383>
- Zhang, Y., Song, C., Band, L. E., & Sun, G. (2019). No proportional increase of terrestrial gross carbon sequestration from the greening Earth. *Journal of Geophysical Research: Biogeosciences*, 124(8), 2540–2553. <https://doi.org/10.1029/2018jg004917>
- Zhang, Y., Song, C., Band, L. E., Sun, G., & Li, J. (2017). Reanalysis of global terrestrial vegetation trends from MODIS products: Browning or greening? *Remote Sensing of Environment*, 191, 145–155. <https://doi.org/10.1016/j.rse.2016.12.018>
- Zhang, Y., Song, C., Sun, G., Band, L. E., McNulty, S., Noormets, A., et al. (2016). Development of a coupled carbon and water model for estimating global gross primary productivity and evapotranspiration based on eddy flux and remote sensing data. *Agricultural and Forest Meteorology*, 223, 116–131. <https://doi.org/10.1016/j.agrformet.2016.04.003>
- Zhang, Y., Song, C., Zhang, K., Cheng, X., Band, L. E., & Zhang, Q. (2014). Effects of land use/land cover and climate changes on terrestrial net primary productivity in the Yangtze River Basin, China, from 2001 to 2010. *Journal of Geophysical Research: Biogeosciences*, 119(6), 1092–1109. <https://doi.org/10.1002/2014JG002616>
- Zhang, K., Song, C., Zhang, Y., & Zhang, Q. (2017). Natural disasters and economic development drive forest dynamics and transition in China. *Forest Policy and Economics*, 76, 56–64. <https://doi.org/10.1016/j.forpol.2015.08.010>
- Zhang, J., Zhang, Y., Sun, G., Song, C., Dannenberg, M. P., Li, J., et al. (2021). Vegetation greening significantly reduced the capacity of water supply to China's South-North water diversion project (pp. 1–28). 2021. <https://doi.org/10.5194/hess-2021-240>
- Zhao, L., Dai, A., & Dong, B. (2018). Changes in global vegetation activity and its driving factors during 1982–2013. *Agricultural and Forest Meteorology*, 249, 198–209. <https://doi.org/10.1016/j.agrformet.2017.11.013>
- Zhou, G., Wei, X., Chen, X., Zhou, P., Liu, X., Xiao, Y., et al. (2015). Global pattern for the effect of climate and land cover on water yield. *Nature Communications*, 6(1), 1–9. <https://doi.org/10.1038/ncomms6918>

- Zhou, S., Yu, B., Huang, Y., & Wang, G. (2014). The effect of vapor pressure deficit on water use efficiency at the subdaily time scale. *Geophysical Research Letters*, 41(14), 5005–5013. <https://doi.org/10.1002/2014GL060741>
- Zhu, Z., Piao, S., Myneni, R. B., Huang, M., Zeng, Z., Canadell, J. G., et al. (2016). Greening of the Earth and its drivers. *Nature Climate Change*, 6(8), 791–795. <https://doi.org/10.1038/nclimate3004>